Journal of Electrochemistry

Volume 23
Issue 2 *Special Issue in Honor of Professor Zhaowu Tian on His 90th Birthday*

2017-04-28

Novel Composites between Nano-Structured Nickel Sulfides and Three-Dimensional Graphene for High Performance Supercapacitors

Xiaomin Wang
College of Materials Science and Engineering, Taiyuan University of Technology, Taiyuan 030024, China;,
wangxiaomin@tyut.edu.cn

Huanglin Dou

Zhen Tian

Jiujun Zhang
College of Science, and Institute for Sustainable Energy, Shanghai University, Shanghai 200444, China;,
jiujun@shaw.ca

Recommended Citation

Xiaomin Wang, Huanglin Dou, Zhen Tian, Jiujun Zhang. Novel Composites between Nano-Structured Nickel Sulfides and Three-Dimensional Graphene for High Performance Supercapacitors[J]. *Journal of Electrochemistry*, 2017 , 23(2): 217-225.
DOI: 10.13208/j.electrochem.161246
Available at: https://jelectrochem.xmu.edu.cn/journal/vol23/iss2/11

DOI: 10.13208/j.electrochem.161246 **Artical ID**:1006-3471(2017)02-0217-09
Cite this: *J. Electrochem.* **2017**, *23*(2): 217-225 **Http**://electrochem.xmu.edu.cn

Novel Composites between Nano-Structured Nickel Sulfides and Three-Dimensional Graphene for High Performance Supercapacitors

Xiaomin Wang[1*], Huanglin Dou[1], Zhen Tian[1], Jiujun Zhang[2*]
(1. *College of Materials Science and Engineering, Taiyuan University of Technology, Taiyuan* 030024, *China*;
2. *College of Science, and Institute for Sustainable Energy, Shanghai University, Shanghai* 200444, *China*)

Abstract: In this paper, a three-dimensional graphene (3DG) network grown on nickel foam was employed as a template for synthesizing graphene-based composite materials of supercapacitor electrode. The composites (crystal Ni_3S_2 nanorods on the surface of 3DG (abbreviated as Ni_3S_2/3DG)) were obtained through a one-step hydrothermal reaction. The morphological and structural evolution of the Ni_3S_2/3DG composites were investigated by SEM, TEM, XRD and Raman spectroscopy. Detailed electrochemical characterization showed that the Ni_3S_2/3DG-coated electrodes exhibited both a specific capacitance as high as 1825 $F \cdot g^{-1}$ at 5 $mV \cdot s^{-1}$ and a discharge capacitance as high as 517 $F \cdot g^{-1}$ at 10 mA. Remarkably, a high cycling performance (~ 100% capacitance retention after 1000 cycles) is achieved at a current density of 20 mA.

Key words: three-dimensional graphene; nickel sulfide; supercapacitor; electrochenical energy storage
CLC Number: TQ150 **Document Code**: A

As a new-type of energy storage devices, supercapacitors have drawn much attention to researchers worked in electrochemical energy storage and conversion due to their extreme high power density and long cycle life when compared to batteries and fuel cells, which have shown great potential applications for portable electronics, electrical vehicles, and so on[1-3]. However, one of the major disadvantages for commercial applications is low energy density, which limits their practical applications where high energy density is required[4]. Therefore, great efforts have been made to improve energy density by using novel electrode materials with high values of specific capacitance and electrolytes with wide voltage windows[5-6]. Regarding electrode materials of supercapacitors, considerable work has been done to develop a variety of active electrode materials, such as transition metal sulfides, carbon-based materials and conducting polymers[7-9].

Transition metal sulfides and their compounds, used for many applications including magnetization, ceramic toughener and hydrogenation catalysts, have been explored for high-performance supercapacitors in recent years because of their low cost, low toxicity, and great flexibility in structure and morphology[10-13]. However, these materials normally have either low conductivity or poor electrochemical stability, which may limit their widespread applications in supercapacitors.

To make transition metal sulfides being suitable for supercapacitor application, combining them with high conductivity material, such as metal nanoparticles, conducting polymers, or carbon materials including graphene, has been explored[14-16]. In the most recent years, graphene-based materials have been identified as excellent conductive matrix materials for anchoring nanoparticles[17-18]. In particular, 3D-graphene (abbreviated as 3DG), which can facilitate ion

Received: 2016-12-07, Revised: 2017-03-03 *Corresponding author, Tel: (86-21)66133250, E-mail: wangxiaomin@tyut.edu.cn; jiujun@shaw.ca

transport by providing a smaller resistance and shorter diffusion pathway, is strongly recommended for the fabrication of advanced supercapacitors. However, the conductivity of graphene-based materials could be largely compromised by the chemical groups and defects introduced during the synthesis process[19]. Furthermore, the aggregation and restacking of graphene nanosheets during processing could lead to significantly reduced surface areas, making it difficult for ions to gain access to the electrode surfaces. In this paper, with the aim of achieving a high energy density and excellent cycle life, a simple, one-step, and cost effective chemical synthesis method was explored for synthesizing composites consisted of nickel sulfide and 3DG. By optimizing the temperature and time, a coaxially-coated nickel sulfide onto 3DG surface was achieved. The materials showed high capacitances, demonstrating that they are the feasible materials for supercapacitor applications.

1 Experimental

1.1 Materials

Nickel foams (0.5 mm thick) were purchased from Alantum Advanced Technology Materials, China. Argon, hydrogen and methane were purchased from Taiyuan Fujiang gas Co., Ltd., China. Ethanol, Thioacetamide (TAA, C_2H_5NS) and potassium hydroxide were supplied from Sinopharm chemical reagent Co., Ltd., China. The water used throughout all experiments was deionized (DI) water purified through a Millipore system.

1.2 Preparation of 3DG/Ni

Nickel foams (~ 30 mg·cm^{-2} in areal density) were used as 3D scaffold templates for the CVD growth of graphene. They were cut into pieces of 3 × 2 cm^2 and placed in a quartz tube, then heated to 1000 ℃ in a tube furnace (KTL1700) at a 10 ℃·min^{-1} heating rate under Ar (500 sccm) and H_2 (200 sccm), and maintained for 10 minutes to remove the surface oxide layer of nickel foam. A small amount of CH_4 was then introduced into the quartz tube with a flow rate of 7 sccm. After 10 minutes of reaction-gas mixture flow, the samples were rapidly cooled to room temperature at a rate of 100 ℃·min^{-1}. Then 3DG/Ni was obtained.

1.3 Preparation of Ni_3S_2/3DG Composite

The Ni_3S_2/3DG composite was synthesized by a simple one-step hydrothermal process. First, the above obtained 3DG/Ni was cut into small pieces of 2 cm × 1 cm. For a typical synthesis, a piece of 3DG/Ni was wrapped with polytetrafluoroethylene sealing tape with exposure area of 1 cm^2. Then putting it into a Teflon-lined stainless-steel autoclave containing 25 mg TAA of 20 mL homogeneous solution. The autoclave was then sealed and heated at 180 ℃ for 3, 6, 12 or 24 hours . After the autoclave was cooled down to room temperature, the sample was removed and washed with ethanol and DI water, then dried at 60 ℃ for 12 hours in vacuum. Then the Ni_3S_2/3DG composite was obtained.

1.4 Material Characterizations

X-ray diffraction (XRD) system (Tongda, TD-3500) was used for the structural analysis. Step scanning was done with 2θ intervals from 10° to 70°. Field emission scanning electron microscope (FESEM, TSCAN, Mira3-LMH) and transmission electron microscope (TEM, JEM 2100F, JEOL) were used to observe the morphology and microstructural characteristics of the synthesized samples. Energy disper sive spectroscope (EDS, TSCAN, Mira3-LMH) and X-ray photoelectron spectroscope (XPS, Amicus Budget) were used to investigate the chemical composition. Raman spectroscope (WITEC, CRM200) was used to analyze the quality and number of layers of 3DG.

1.5 Electrochemical Measurements

All the electrochemical measurements were car ried out with an electrochemical analyzer (CHI 660D work station, CH Instruments, Inc. USA) using a three-electrode system in 3 mol·L^{-1} KOH electrolyte solution under ambient conditions. The electrode potentials were measured with respect to a reference electrode of Hg/Hg_2Cl_2 (saturated KCl). Pt wire was used as the counter electrode. The cyclic voltammetric measurements were performed at various scan rates in the potential range from -0.2 to 0.7 V.

2 Results and Discussion

The morphology of the 3DG foam was examined by SEM, as shown in Fig.1A. After removal of the Ni template, graphene was remained, keeping the 3D network and the porous structure of the compressed Ni foam without collapsing and cracking. The width of the graphene skeleton was about 100 to 120 μm. Fig. 1B shows the XRD pattern of 3DG. A large diffraction peak was observed at 2θ = 26.5°, which can be attributed to the (002) reflection of graphitic carbon. Fig. 1C shows the Raman spectrum of 3DG. Except for the characteristic of graphene and 2D peaks at ~ 1577.3 cm^{-1} and 2725.7 cm^{-1}, in addition, there was a weak grapheme D band at ~ 1350 cm^{-1}, indicating that the graphene foam is of high quality, that is, lack of defects[20]. The integral ratio of the 2D and G band indicates that the as-grown graphene foams consist of mainly one- to few-layered domains. This result was in accordance with the SEM observation.

In order to explore the morphological and structural evolution of Ni_3S_2/3DG in a series of experiments with different hydrothermal reaction time, four samples prepared with different time were examined by SEM, as shown in Fig. 2. It can be observed that when the hydrothermal reaction time was 3 hours, an irregular rod-like structure of Ni_3S_2 sample with diameters between 100 to 250 nm can be seen from Fig. 2A. After a hydrothermal reaction time of 6 hours, both the density and sample size were increased (Fig. 2B). When the hydrothermal reaction was carried out for 12 hours, the irregular block structure sample was observed. The diameter of the sample varied from 400 to 600 nm (Fig. 2C). Fig. 2D is the SEM image of the sample at a longer reaction time of 24 hours. The rod-like structure disappeared entirely[21].

Fig. 3 shows the XRD spectra of the as-grown Ni_3S_2/3DG at different conditions and it can be seen that the peak intensity of Ni_3S_2 was slightly increased with the reaction time extending. The identified peaks of Ni_3S_2/3DG composite at 2θ = 21.7°, 31.1°, 37.8°, 49.7° and 55.2° corresponded to the (101), (110), (003), (113) and (122) faces of Ni_3S_2 (JCPDS No. 44-1418), respectively. The peaks at 2θ = 44.5° and 51.8° corresponded to the (111) and (200) of the Ni crystals located at the Ni foam substrate (JCPDS No. 65-2865)[18]. The diffraction peaks of Ni_3S_2/3DG composite showed the feature of broadening, which indicates the well crystalized structure. The results were concordant to the SEM analysis, as well as the TEM analysis to be given below.

The nanostructure of Ni_3S_2 nanorods was further investigated using TEM. Fig. 4A shows an individual Ni_3S_2 nanorod on the 3DG substrate film. It can be seen that there were some flake structured particles on the 3DG surface with a diameter of about 100 nm. Fig. 4B image was taken by selecting a certain position in Fig. 4A with a further enlarged observation. The image obtained from the white square area in Fig. 4B with a lattice spacing of 0.28 nm in the backbone area of the Ni_3S_2 nanorod, which corresponds to the (110) interplanar spacing of Ni_3S_2[22-23]. In addition, the energy dispersive X-ray spectrometric (EDS) analysis was conducted to confirm the composition of Ni_3S_2 (Fig. 4C).

In order to further confirm the chemical compositions of the Ni_3S_2/3DG composite, X-ray photoelectron spectroscopic (XPS) measurements were performed in the region of 0 ~ 1000 eV for the samples pre-

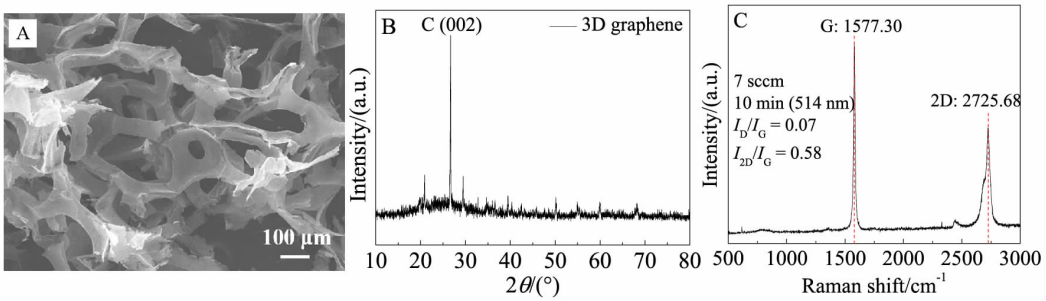

Fig. 1 SEM image (A), XRD pattern (B), and Raman spectrum (C) of 3DG

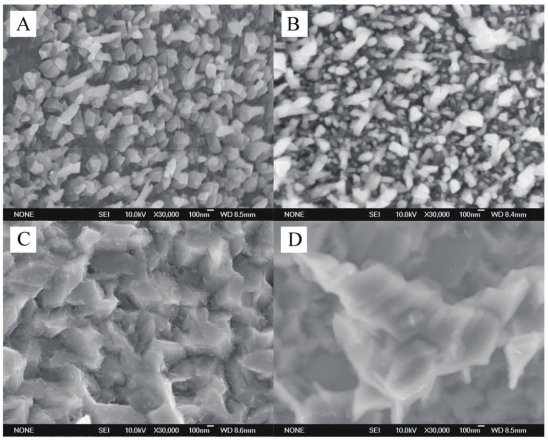

Fig. 2 SEM images of Ni_3S_2/3DG prepared with different reaction time

A. 3 hours; B. 6 hours; C. 12 hours; D. 24 hours

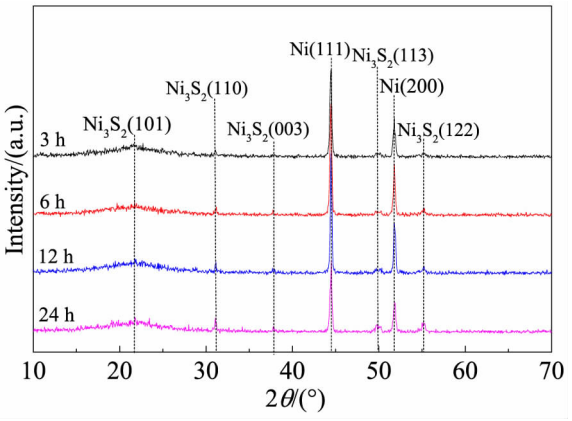

Fig. 3 XRD patterns of Ni_3S_2/3DG prepared with different reaction time

pared with different hydrothermal reaction time, namely, 3, 6, 12 and 24 hours. The XPS spectra of the Ni_3S_2/3DG composite are given in Fig. 5(A-L), which mainly show nickel (Fig. 5(A-D)), sulfur (Fig. 5(E-H)) and carbon (Fig. 5(I-L)) species with four different reaction time. For the four samples prepared with different reaction time, the XPS spectra of Ni 2p in Fig. 5A-D all exhibited four main peaks. The peaks at 855.2 eV and 873.7 eV corresponded to $Ni(OH)_2$ Ni $2p_{3/2}$ and Ni $2p_{1/2}$, respectively, with a spin-energy separation of 17.6 eV. The peaks at 852.8 eV and 870.6 eV corresponded to Ni_3S_2, Ni $2p_{3/2}$ and Ni $2p_{1/2}$, respectively, with a spin energy separation of 17.8 eV[8, 24]. The XPS spectra of S2p in Fig. 5(E-H) displayed peaks at 162.3 eV, 162.5 eV, 162.0 eV, and 168.0 eV. The peaks located at 284.8 eV in C 1s spectra of grapheme corresponding to C—C are shown in Fig. 5(I-L) for the four samples with different reaction time, indicating that graphene exists in all the samples, which is consistent with the result from the

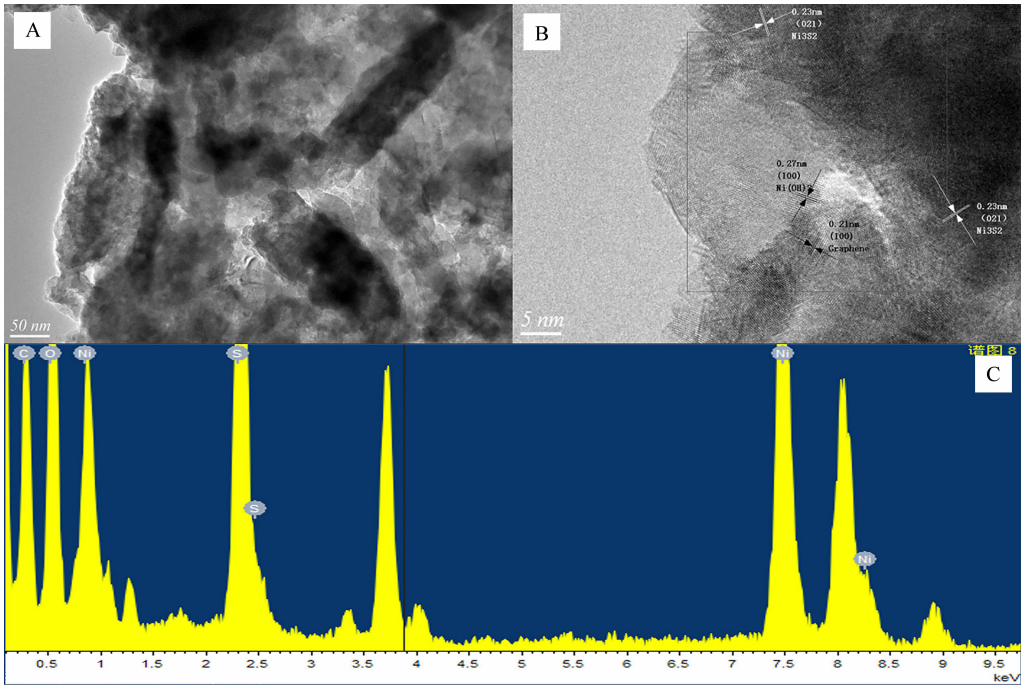

Fig. 4 High resolution TEM image (A), Lattice fringe image (B), and EDS pattern (C) of Ni_3S_2/3DG

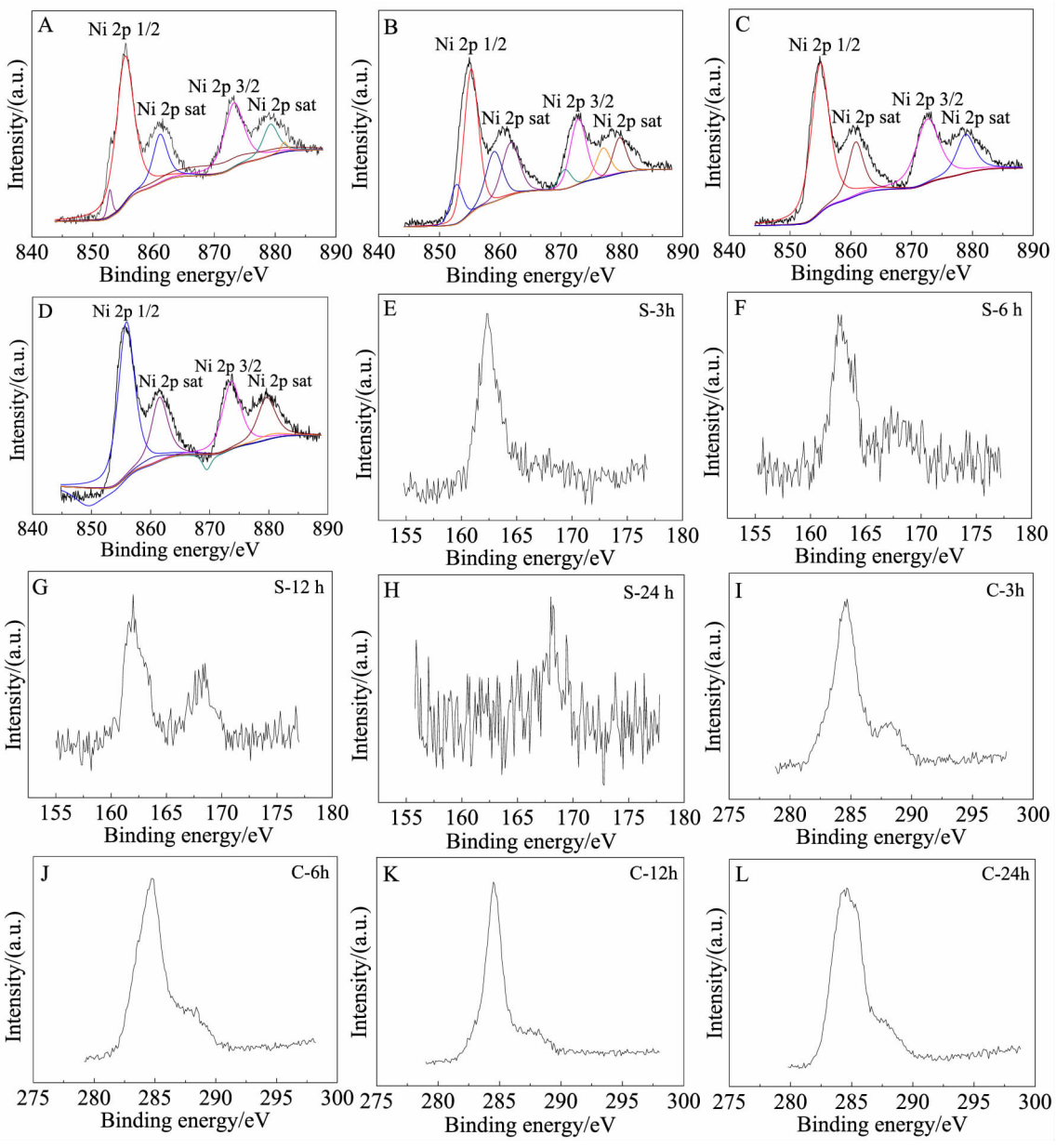

Fig. 5 XPS spectra of Ni 2p (A-D), S2p (E-H) and C1s (I-L) the for Ni_3S_2/3DG composite prepared with various reaction time

Raman spectra (not shown). These XPS results confirm the presence of Ni_3S_2 in all the samples synthesized at different reaction time, which is also consistent with the XRD results. The results demonstrate that the Ni_3S_2/3DG composite samples have been successfully synthesized.

Fig. 6A shows the cyclic voltammograms (CVs) of the Ni_3S_2/3DG samples coated electrode recorded at a scan rate of 5 mV·s^{-1}. All of the CV curves exhibited a pair of redox peaks, which are distinguishable from those of electric double-layer capacitors, implying the presence of reversible Faradaic reaction. The specific capacitance values of the Ni_3S_2/3DG samples prepared with 3, 6, 12 and 24 hours were calculated to be 1270, 1355, 1825 and 772 F·g^{-1}, respectively. The Ni_3S_2/3DG-12 h electrode was the highest among the samples studied. This indicates that the 3DG-composited Ni_2S_2 on the surface of nickel foam played an role in enhancing the supercapacitor performance[25-27]. Combined with the SEM analysis, this enhanced electrochemical performance due to the surface of Ni_3S_2/3DG obtained at 12 hours

was much more smooth, which could reduce the distance of electron transport and increase the rate of Faradaic reaction.

Fig.7A shows the comparison of galvanostatic charge-discharge (GCD) curves for the samples at a current density of 10 mA·cm^{-2}. The specific capacitance, C_m, (listed in Table 2) can be calculated using the following equation:

$$C_m = \frac{I \times \Delta t}{m \times \Delta V} \quad (1)$$

where ΔV(V) is the potential window, I(A) is the charge-discharge current, Δt(s) is the discharge time, and m(g) is the mass of an active material.

From Table 1, it can be seen that the Ni_3S_2/3DG-12 h electrode could deliver the highest specific capacitance of 516 F·g^{-1}. To further understand the rate capability and the electrochemical capacitive properties of the composite electrodes, the galvanostatic charge-discharge measurements were carried out at various current densities of 10, 20, 40 and 80 mA·cm^{-2} (Fig. 7B). The Cm values of Ni_3S_2/3DG-12 h electrode at 10 and 80 mA·cm^{-2} were 516.7 and 373.7 F·g^{-1}, respectively, which are much higher than those of 3, 6 and 24 hours electrodes at the same current density. About 90.4% of the C_m could be retained when the current density was increased from 10 to 80 mA·cm^{-2}. The specific capacitance was gradually decreased with increasing the current density due to the increment of voltage drop and the insufficient active material involved in redox reaction at higher current density. However, the Ni_3S_2/3DG-12 h electrode possessed an excellent capacitance with all the current densities and showed a good rate capability. This might be due to the 3D structure of electrode allowing rapid transportation of electrolyte ions, which then improved the rate capability of the electrodes. The high performance of electrode over a wide range of large current densities confirmed that it was a promising electrode material[28]. As shown in Fig. 7E, the cycling test was carried out for one thousand cycles at 20 mA·cm^{-2}. The Ni_3S_2/3DG-12h electrode exhibits excellent cycle stability in the entire cycle numbers. After 200 cycles, the capacitance of the Ni_3S_2/3DG-12 h electrode increased 7% of its initial value, then remained stable capacitance till the end, demonstrating that the Ni_3S_2/3DG-12 h electrode possessed a long-term electrochemical stability.

In order to further investigate the electrochemical conductivity behavior of the Ni_3S_2/3DG electrodes, an electrochemical impedance spectroscopic (EIS) analysis was conducted in a frequency ranging from 0.01 Hz to 100 kHz, as shown in Fig. 7D. The impedance plots include a high frequency component (partial semicircle), a low-frequency component (straight slopping line along the imaginary axis) and a transition zone between two regions. The impedance curve can be explained by an equivalent Randles circuit that includes solution resistance, double layer capacitance, charge transfer resistance, and Warburg impedance. The intercept with the real axis at very high frequency represents a combined resistance (R_s) including intrinsic resistance of the active material and the binder in the electrodes, ionic resistance of

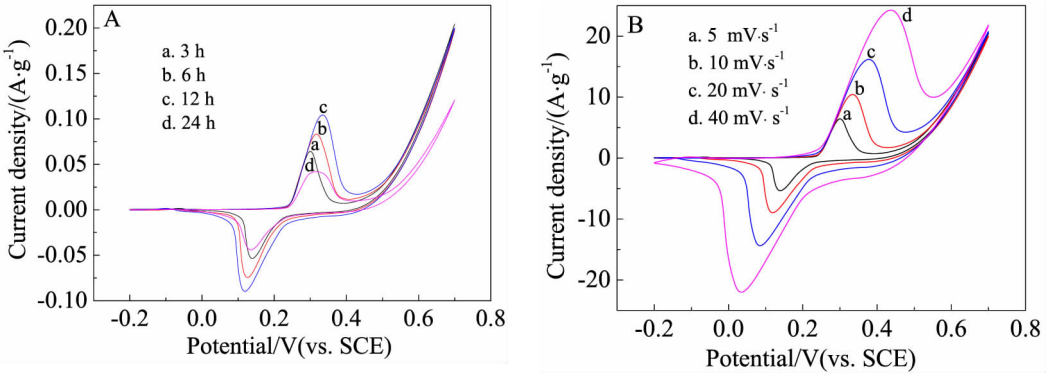

Fig. 6 A. Cyclic voltammograms of composite electrodes measured at a scan rate of 5 mV·s^{-1}; B. Cyclic voltammograms of Ni_3S_2/3DG-12 h electrode at various scan rates

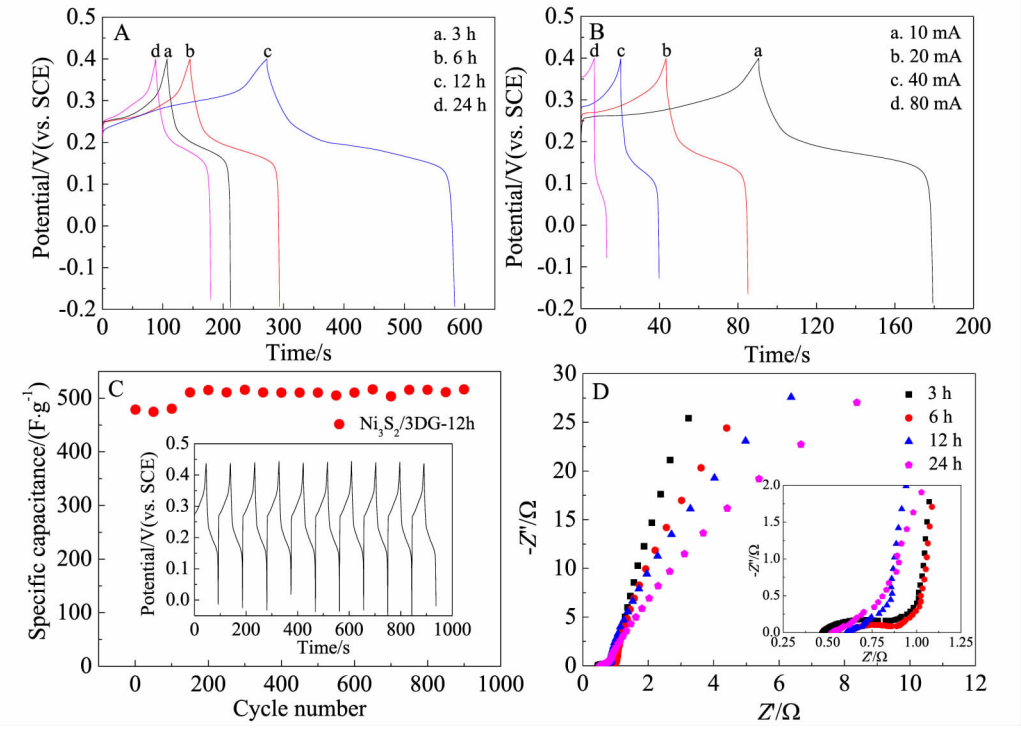

Fig. 7 Electrochemical performances of the composite electrodes

A. GCD curves at a current density of 10 mA·cm^{-2} of the composite electrodes; B. GCD plots at various current densities of Ni_3S_2/3DG-12 h electrode; C. Cycling performance of Ni_3S_2/3DG-12 h electrode at a current density of 20 mA·cm^{-2}; D. EIS plots of the composite electrodes in the frequency range from 100 kHz to 0.01 Hz. Inset: expanded views of the high frequency region displayed in the right part.

Tab. 1 Electrochemical performance parameters of the composite electrodes at 5 mV·s^{-1}

Parameter	Ni_3S_2/3DG-3 h	Ni_3S_2/3DG-6 h	Ni_3S_2/3DG-12 h	Ni_3S_2/3DG-24 h
C_m(CV)/(F·g^{-1})	1270.6	1355.1	1825.3	772.4
C_m(GCD)/(F·g^{-1})	203.7 (10 mA·cm^{-2}); 148.1 (80 mA·cm^{-2})	277.8 (10 mA·cm^{-2}); 251.4 (80 mA·cm^{-2})	516.7 (10 mA·cm^{-2}); 373.3 (80 mA·cm^{-2})	157.7 (10 mA·cm^{-2}); 112.3 (80 mA·cm^{-2})
R_{ct}/Ω	0.4	0.5	0.6	0.6
Rate capability	72.7%	90.4%	72.2%	71.2%

the electrolyte, and contact resistance at the interface active material and current collector. It can be seen that, the charge transfer resistance (R_{ct}) of Ni_3S_2/3DG-12 h electrode was much smaller than those of others, which means the easier electron transport[29]. It also showed a more vertical line than other electrodes at low frequency, which illustrates that the electrode had a smaller Warburg impedance (W_s), meaning that the ion diffusion in the solution and the adsorption of ions onto the electrode surface occurred more swiftly. It could be explained that the existence of 3DG in electrode provides easy access and more space for electrolyte diffusion. The small bulk resistance, interfacial charge transfer resistance and Warburg impedance all indicated that the Ni_3S_2/3DG-12 h electrode was a high-performing material for supercapacitor.

3 Conclusions

In summary, the Ni_3S_2/3DG electrode materials were synthesized by a simple one step hydrothermal reaction. By controlling the reaction time, different nanostructured Ni_3S_2/3DG samples were obtained.

Detailed electrochemical characterization showed that the Ni_3S_2/3DG, in particular, Ni_3S_2/3DG-12 h, exhibited a high specific capacitance (1825 $F \cdot g^{-1}$ at 5 $mV \cdot s^{-1}$) and a discharge capacitance (516.7 $F \cdot g^{-1}$ at 10 mA) with high cycling performance (almost 100% capacitance retention after 1000 cycles). The enhanced supercapacitor performance might arise from the synergistic effect between Ni_3S_2 nanorods and 3DG network.

Acknowledgements:

This work was supported by the National Natural Science Foundation of China (Grant No. 51372160 and 51172152).

References:

[1] Zhang C, He X J, Li G R, Reduced graphene oxide (RGO) hollow network cages for high-performance electrochemical energy storage[J]. Journal of Electrochemistry, 2016, 22(3): 278-287.

[2] Zhong C, Deng Y D, Hu W B, et al. A review of electrolyte materials and compositions for electrochemical supercapacitors[J]. Chemical Society Reviews, 2015, 44: 7484-7539.

[3] Su X, Yu L, Cheng G, et al. Controllable hydrothermal synthesis of Cu-doped δ-MnO_2 films with different morphologies for energy storage and conversion using supercapacitors[J]. Applied Energy, 2014, 134: 439-445.

[4] Ambrosi A, Chua C K, Bonanni A, Pumera M. Electrochemistry of graphene and related materials[J]. Chemical Reviews, 2014, 114(14): 7150-7188.

[5] Ghosh D, Das C K. Hydrothermal growth of hierarchical Ni_3S_2 and Co_3S_4 on a reduced graphene oxide hydrogel@Ni foam: A high-energy-density aqueous asymmetric supercapacitor[J]. ACS Applied Materials & Interfaces, 2015, 7: 1122-1131.

[6] Zhao B, Jiang L, Yuen M H, et al. Electrochemical syntheses of graphene and composites[J]. Journal of Electrochemistry, 2016, 22(1): 1-19.

[7] Banerjee P C, Lobo D E, Middag R, et al. Electrochemical capacitance of Ni-doped metal organic framework and reduced graphene oxide composites: More than the sum of its parts [J]. ACS Applied Materials & Interfaces, 2015, 7(6): 3655-3664.

[8] Liu Y, Wang R, Yan X. Synergistic effect between ultra-small nickel hydroxide nanoparticles and reduced graphene oxide sheets for the application in high-performance asymmetric supercapacitor[J]. Scientific Reports, 2015, 5: 11095.

[9] Jiang W, Yu D, Zhang Q, et al. Ternary hybrids of amorphous nickel hydroxide-carbon nanotube-conducting polymer for supercapacitors with high energy density, excellent rate capability, and long cycle life[J]. Advanced Functional Materials, 2015, 25(7): 1063-1073.

[10] Yang B, Yu L, Liu Q, et al. The growth and assembly of the multidimensional hierarchical Ni_3S_2 for aqueous asymmetric supercapacitors[J]. CrystEngComm, 2015, 17: 4495-4501.

[11] Salunkhe R R, Lin J, Malgras V, et al. Large-scale synthesis of coaxial carbon nanotube/$Ni(OH)_2$ composites for asymmetric supercapacitor application[J]. Nano Energy, 2015, 11: 211-218.

[12] Cao X, Yin Z, Zhang H. Three-dimensional graphene materials: Preparation, structures and application in supercapacitors [J]. Energy & Environmental Science, 2014, 7: 1850-1865.

[13] Li H, Yang X W, Wang X M, et al. A dual-spatially-confined reservoir by packing micropores within dense graphene for long-life lithium/sulfur batteries[J]. Nanoscale, 2016, 8: 2395-2402.

[14] Zhang Z, Wang Q, Zhao C, et al. One-step hydrothermal synthesis of 3D petal-like Co_9S_8/RGO/Ni_3S_2 composite on nickel foam for high-performance supercapacitors[J]. ACS Applied Materials & Interfaces, 2015, 7(8): 4861-4618.

[15] Ramachandran R, Saranya M, Velmurugan V, et al. Effect of reducing agent on graphene synthesis and its influence on charge storage towards supercapacitor applications [J]. Applied Energy, 2015, 153: 22-31.

[16] Zhang Z, Liu X, Qi X, et al. Hydrothermal synthesis of Ni_3S_2/graphene electrode and its application in a supercapacitor[J]. RSC Advances, 2014, 4: 37278.

[17] Xu Y, Huang X, Lin Z, et al. One-step strategy to graphene/$Ni(OH)_2$ composite hydrogels as advanced three-dimensional supercapacitor electrode materials[J]. Nano Research, 2012, 6(1): 65-76.

[18] Yan H, Bai J, Wang B, et al. Electrochemical reduction approach-based 3D graphene/$Ni(OH)_2$ electrode for high-performance supercapacitors[J]. Electrochimica Acta, 2015, 154: 9-16.

[19] Mao S, Lu G, Chen J. Three-dimensional graphene-based composites for energy applications[J]. Nanoscale, 2015, 7: 6924-6943.

[20] Philip M R, Narayanan T N, Praveen Kumar M, et al. Self-protected nickel-graphene hybrid low density 3D scaffolds[J]. Journal of Materials Chemistry A, 2014, 45:

19488-19494.

[21] Zhang Z, Huang Z, Ren L, et al. One-pot synthesis of hierarchically nanostructured Ni_3S_2 dendrites as active materials for supercapacitors[J]. Electrochimica Acta, 2014, 149: 316-323.

[22] Yu W, Lin W, Shao X, et al. High performance supercapacitor based on Ni_3S_2/carbon nanofibers and carbon nanofibers electrodes derived from bacterial cellulose[J]. Journal of Power Sources, 2014, 272: 137-143.

[23] Zhou W, Cao X, Zeng Z, et al. One-step synthesis of Ni_3S_2 nanorod@$Ni(OH)_2$ nanosheet core-shell nanostructures on a three-dimensional graphene network for high-performance supercapacitors[J]. Energy & Environmental Science, 2013, 6: 2216-2221.

[24] Li M, Tang Z, Leng M, et al. Flexible solid-state supercapacitor based on graphene-based hybrid films[J]. Advanced Functional Materials, 2014, 24(47): 7495-7502.

[25] Wang Y, Wu G C, Wang Y Z, et al. Effect of water content on the ethanol electro-oxidation activity of Pt-Sn/graphene catalysts prepared by the polyalcohol method [J]. Electrochimica Acta, 2014, 130: 135-140.

[26] Li G, Xu C. Hydrothermal synthesis of 3D $Ni_xCo_{1-x}S_2$ particles/graphene composite hydrogels for high performance supercapacitors[J]. Carbon, 2015, 90: 44-52.

[27] Nguyen V H, Lamiel C, Shim J J. Hierarchical mesoporous graphene@Ni-Co-S arrays on nickel foam for high-performance supercapacitors[J]. Electrochimica Acta, 2015, 161: 351-357.

[28] Huo H, Zhao Y, Xu C. 3D Ni_3S_2 nanosheet arrays supported on Ni foam for high-performance supercapacitor and non-enzymatic glucose detection[J]. Journal of Materials Chemistry A, 2014, 36: 15111-15117.

[29] Zhou R,Han C J,Wang X M. Hierarchical MoS_2-coated three-dimensional graphene network for enhanced supercapacitor performances[J]. Journal of Power Sources, 2017, 352: 99-110.

硫化镍/三维网络石墨烯复合材料制备及其在高性能超级电容器的应用研究

王晓敏[1*]，窦湟琳[1]，田　真[1]，张久俊[2*]

(1. 太原理工大学材料科学与工程学院，山西 太原；2. 上海大学理学院/可持续能源研究院，上海)

摘要：本文在泡沫镍上生长三维网络状结构的石墨烯(3DG)，以此为模板合成石墨烯复合电极并将其应用于超级电容器. 采用一步水热法在 3DG 上合成得到 Ni_3S_2 纳米棒结构(Ni_3S_2/3DG). 通过 TEM、XRD、SEM 和拉曼光谱等手段表征对 Ni_3S_2/3DG 复合材料的形态与结构进行表征. 电化学测试表明，Ni_3S_2/3DG 复合材料具有高的比电容(在扫速为 5 mV·s^{-1} 下，具有 1825.3 F·g^{-1} 的比容量)和放电电容(在电流密度 10 mA 下电容高达 516.7 F·g^{-1}). 此外，在电流密度 20 mA 下具有良好的循环性能(循环 1000 周后仍能保留约 100%的初始电容). 本工作为得到高能量密度和良好的长期稳定性的复合材料提供了参考.

关键词：三维石墨烯；硫化镍；超级电容器；电化学储能